Journal of Applied Analysis and Computation
Volume 17, Number 1, February 2027, 87–104
Website:http://www.jaac-online.com
DOI:10.11948/20250384

NUMERICAL ANALYSIS OF A BDF2 FINITE ELEMENT SCHEME FOR NAVIER-STOKES-ALPHA MODEL

Hongjian Wang[1] and Shengkun Li[1,†]

Abstract In this paper, we study a second-order backward difference formula (BDF2) scheme for the Navier-Stokes-alpha model. We combine a stabilized finite element discretization in space with the BDF2 method in time to obtain a fully discrete approximation. A complete numerical analysis is presented, establishing unconditional stability and deriving optimal-order error estimates for the scheme. Numerical experiments are provided to verify the theoretical results and to illustrate the effectiveness of the proposed approach.

Keywords Navier-Stokes-alpha model, BDF2 scheme, error analysis.

MSC(2010) 65M06, 65M60.

1. Introduction

The primary rationale behind large-eddy simulation (LES) lies in the observation that, for many engineering applications, it is not essential to resolve the entire spectrum of spatial turbulent scales. In high-Reynolds-number flows, the Kolmogorov K41 theory indicates that the smallest turbulent scales exhibit statistically uniform and isotropic behavior [14]. Consequently, regularization techniques for the Navier–Stokes equations (NSE) have been developed to explicitly resolve only those scales above a certain physically significant threshold, while modeling the collective influence of the unresolved subgrid scales [18]. Among these regularizations, the Navier–Stokes-α (NS-α) model, also known in the literature as the Camassa–Holm equations, was originally introduced as a turbulence closure model. Its formulation combines a Lagrangian-averaged dispersive nonlinearity with classical Newtonian viscosity [23].

The effectiveness of the NS-α model as an LES framework stems largely from its mathematical consistency with fundamental phenomenological properties of turbulent flows. Beyond being frame-invariant [10], the model has been shown to preserve a quantity analogous to energy and helicity [16]. Although numerical approximations based on turbulence models frequently struggle to retain the full physical fidelity of the continuous equations, carefully designed discretizations of the NS-α model can preserve analogous invariants: In two dimensions, quantities corresponding to energy and enstrophy; in three dimensions, a model-energy and the exact helicity [24]. These favorable properties have spurred the development of a family of related α-type models. Two notable examples are the Navier–Stokes-ω (NS-ω) model, which applies smoothing to the vorticity in the convective term [15], and the multiscale Navier–Stokes-α-ω (NS-α-ω) model, an extension designed to recover flow scales that may be excessively damped by over-regularization [7].

[†]The corresponding author.
[1]College of Applied Mathematics, Chengdu University of Information Technology, Chengdu, Sichuan 610225, China
Email: wanghongjian992@gmail.com(H. Wang), lishengkun@cuit.edu.cn(S. Li)

In the α-model framework, the convective term is expressed in rotational form. For the NS-α model, this leads to the following system:

$$u_t - \bar{u} \times (\nabla \times u) + \nabla p - \nu \Delta u = f, \tag{1.1}$$

$$\nabla \cdot \bar{u} = 0, \tag{1.2}$$

$$-\alpha^2 \Delta \bar{u} + \bar{u} = u. \tag{1.3}$$

Here, $u = u(x,t)$ denotes the velocity field, $p = p(x,t)$ the pressure, ν the kinematic viscosity, and $f = f(x,t)$ a given external force. The filtering operation is defined via the Helmholtz filter $(-\alpha^2 I + I)^{-1}$, where $\alpha > 0$ is the filtering radius. The system is posed on a bounded polyhedral domain $\Omega \subset \mathbb{R}^d$ $(d = 2, 3)$, supplemented with suitable initial conditions and the no-slip boundary condition $u = 0$ on $\partial\Omega$. A detailed discussion of the mathematical theory for the continuous NS-α model can be found in [17].

Numerical challenges. Developing efficient and accurate numerical methods for the NS-α model presents several significant challenges that distinguish it from the classical Navier–Stokes equations:

(i) **Rotational nonlinearity:** The convective term $\bar{u} \times (\nabla \times u)$ involves the filtered velocity $\bar{u}$ rather than the primitive variable u, requiring careful treatment of the coupling between the momentum equation and the filter equation.

(ii) **Stability requirements:** The rotational form, while preserving physical invariants, requires specialized temporal discretization strategies to maintain unconditional stability without excessive time-step restrictions.

(iii) **Filtering-discretization coupling:** The discrete filter must be compatible with the finite element spaces to preserve the stability and accuracy properties of the continuous model.

Critical review of existing methods. Numerical methods for approximating the NSE have been extensively studied, encompassing techniques such as backward difference formulas, projection methods, and discontinuous Galerkin schemes. For instance, Li et al. [20] proposed a second-order mixed stabilized finite element method for the variable-density Navier–Stokes equations, employing a second-order backward difference (BDF2) scheme for temporal discretization. Dokken and Johansson [6] introduced a second-order projection method that combines the BDF2 scheme for time stepping with finite elements in space, providing numerical experiments to verify convergence. Li and Shen et al. [21] developed a scalar auxiliary variable (SAV) approach, which yields unconditionally stable schemes for the NSE along with rigorous error estimates.

However, existing work on the NS-α model has primarily focused on:

- Spatial discretization schemes without rigorous temporal error analysis [13, 24].
- First-order temporal schemes that suffer from accuracy limitations for long-time simulations.
- Stabilization techniques that introduce additional numerical dissipation.

Notably, a rigorous convergence analysis of second-order BDF schemes for the NS-α model remains absent from the literature. This gap is significant because:

- Second-order methods are essential for efficient long-time turbulence simulations.

- The coupling between the BDF2 temporal discretization and the Helmholtz filter requires careful analysis.
- The rotational nonlinearity presents unique challenges for stability proofs that differ from the standard convective form.

Novel contributions. In the present work, we address these gaps by providing the first rigorous convergence analysis of a fully discrete scheme for the NS-α model that combines the BDF2 method for temporal discretization with finite elements in space. Our specific contributions are:

- **Unconditional stability:** We prove that the proposed BDF2 scheme is unconditionally stable, with no time-step restrictions depending on the mesh size h or the filtering radius α.
- **Optimal error estimates:** We derive optimal-order error estimates of order $O(h^k + (\Delta t)^2 + \alpha^2)$, where k is the polynomial degree of the velocity finite element space.
- **Filtering error control:** Our analysis explicitly accounts for the filtering error and its interaction with the temporal discretization.
- **Comprehensive numerical validation:** We verify the theoretical convergence rates and demonstrate the effectiveness of the scheme on a challenging benchmark problem.

Multi-step backward difference formulas (BDF) are widely adopted for time integration of partial differential equations [3, 4, 19, 22, 25, 28]. Among them, the BDF2 scheme is particularly popular due to its favorable stability and accuracy properties [2]. The analysis of first- and second-order BDF time semi-discretizations for the Navier–Stokes equations was pioneered by Girault and Raviart [9]. More recently, Rebholz and Tone [26] established long-time H^1-stability of the BDF2 scheme for the two-dimensional NSE, while Rong and Fiordilino [27] introduced and analyzed a BDF2-based modular grad-div stabilization method. To the best of our knowledge, however, a rigorous convergence analysis of the BDF2 scheme applied to the NS-α model remains absent from the literature. This gap motivates the current study.

The structure of the paper is organized as follows. Section 2 introduces the necessary notation and collects preliminary results that will be used throughout the analysis. In Section 3, we present the fully discrete BDF2 finite element scheme for the NS-α model, followed by a detailed investigation of its unconditional stability. Section 4 is devoted to a rigorous error analysis, where optimal-order error estimates are established under reasonable regularity assumptions. Finally, in Section 5, we conduct several numerical experiments to validate the theoretical results and demonstrate the effectiveness of the proposed scheme.

2. Notation and preliminaries

This section collects the necessary notation, definitions, and preliminary results that will be used throughout the paper. Constants that appear in estimates are generically denoted by C, which may take different values at different occurrences but is always independent of the spatial mesh size h and the time step Δt. We denote by $(\cdot,\cdot)$ and $\|\cdot\|$ the standard $L^2(\Omega)$ inner product and norm, respectively. For $1 \le p \le \infty$, the $L^p(\Omega)$ norm is written as $\|\cdot\|_{L^p}$. Sobolev spaces $W_p^k(\Omega)$ and their norms $\|\cdot\|_{W_p^k}$ are defined in the usual way (see, e.g., [1]). In particular, for

$p = 2$ we write $H^k(\Omega) = W_2^k(\Omega)$ and denote its norm by $\|\cdot\|_k$. The following function spaces will be frequently used:

$$
\begin{aligned}
L^p(0,T;L^s(\Omega)) &:= \left\{ v : [0,T] \to L^s(\Omega) | (\int_0^T \|v(\cdot,t)\|_{L^s}^p dt)^{\frac{1}{p}} < \infty \right\}, \\
L^\infty(0,T;L^s(\Omega)) &:= \left\{ v : [0,T] \to L^s(\Omega) | ess \sup_{0\le t\le T} \|v(\cdot,t)\|_{L^s} < \infty \right\}, \\
L^p(0,T;H^k(\Omega)) &:= \left\{ v : [0,T] \to H^k(\Omega) | (\int_0^T \|v(\cdot,t)\|_k^p dt)^{\frac{1}{p}} < \infty \right\}, \\
L^\infty(0,T;H^k(\Omega)) &:= \left\{ v : [0,T] \to H^k(\Omega) | ess \sup_{0\le t\le T} \|v(\cdot,t)\|_k < \infty \right\}.
\end{aligned}
$$

Here, $1 \le p < \infty, 1 \le s \le \infty, 1 \le r < \infty$. For the function spaces, we have these norms

$$
\begin{aligned}
\|v\|_{p,k} &:= \left(\int_0^T \|v(\cdot,t)\|_k^p dt \right)^{\frac{1}{p}} &&\text{for } v \in L^p(0,T;H^k(\Omega)), \\
\|v\|_{\infty,k} &:= ess \sup_{0\le t\le T} \|v(\cdot,t)\|_k &&\text{for } v \in L^\infty(0,T;H^k(\Omega)).
\end{aligned}
$$

We divide the time interval $[0,T]$ into m elements (t_n, t_{n+1}) for $n = 0, 1, \cdots, m-1$, where $t_n := n\Delta t$ and $\Delta t = \frac{T}{m}$. Next, we introduce the analogous norms in the discrete condition

$$
|||v|||_{p,k} = \left(\Delta t \sum_{n=0}^{m} \|v^n\|_k^p \right)^{\frac{1}{p}}, \qquad |||v|||_{\infty,k} := \max_{0\le n\le m} \|v^n\|_k,
$$

where $v^n = v(t_n)$ and the same goes for the other variables.

Next, we define the velocity and pressure spaces by

$$
\begin{aligned}
X = H_0^1(\Omega) &:= \left\{ v \in H^1(\Omega) : v|_{\partial\Omega} = 0 \right\}, \\
Q = L_0^2(\Omega) &:= \left\{ q \in L^2(\Omega) : \int_\Omega q = 0 \right\},
\end{aligned}
$$

we define X^* is the dual space of X, and the norm is denoted by $\|\cdot\|_*$. Then, the space of divergence-free V is denoted by

$$
V := \{ v \in X : (\nabla \cdot v, q) = 0 \ \forall q \in Q \}.
$$

Next, we define the trilinear form $b(\cdot,\cdot,\cdot)$ and $b_\alpha(\cdot,\cdot,\cdot)$ by

$$
\begin{aligned}
b(u,v,w) &:= ((\nabla \times u) \times \bar{v}, w), \\
b_\alpha(u,v,w) &:= ((\nabla \times u) \times \bar{v}, w),
\end{aligned}
$$

where $\bar{v} = (-\alpha^2\Delta + I)^{-1} v$ denotes the filtered velocity. In the discrete setting, $\bar{v}^h \in X^h$ satisfies the discrete filter equation (2.2), and the discrete trilinear form is defined as

$$
b_\alpha(u^h, v^h, w^h) := ((\nabla \times u^h) \times \bar{v}^h, w^h).
$$

For $u, v, w \in X$, the trilinear form $b(u, v, w)$ satisfies the following inequalities [9,15]:

$$
\begin{aligned}
|b(u, v, w)| &\leq C\|\nabla \times u\|\|v\|_\infty\|w\|, \\
|b(u, v, w)| &\leq C\|\nabla \times u\|_\infty\|v\|\|w\|, \\
|b(u, v, w)| &\leq C\|\nabla \times u\|\|\nabla v\|\|\nabla w\|, \\
|b(u, v, w)| &\leq C\|u\|^{\frac{1}{2}}\|\nabla u\|^{\frac{1}{2}}\|\nabla v\|\|\nabla w\|.
\end{aligned}
$$

The weak formulation of (1.1) is: Find $u : [0, T] \to X$ and $p : [0, T] \to Q$ satisfying

$$
\begin{aligned}
&(u_t, v) + b(u, u, v) + \nu(\nabla u, \nabla v) - (p, \nabla \cdot v) = (f, v) \quad \forall v \in X, \\
&(\nabla \cdot u, q) = 0 \quad \forall q \in Q.
\end{aligned} \tag{2.1}
$$

Here, the trilinear form $b(u, u, v) = ((\nabla \times u) \times \bar{u}, v)$ implicitly incorporates the filtering operation through $\bar{u} = (-\alpha^2\Delta + I)^{-1}u$.

Let $\mathcal{T}_h = \{K\}$ be a family of shape-regular triangulations of Ω, with mesh size $h = \max_{K\in\mathcal{T}_h} h_K$, where h_K denotes the diameter of element K. Associated with $\mathcal{T}_h$, we introduce conforming finite element spaces $X^h \subset X$ and $Q^h \subset Q$ for the velocity and pressure, respectively. The discrete divergence-free subspace is defined as

$$
V^h := \{v^h \in X^h : (\nabla \cdot v^h, q^h) = 0 \ \forall q^h \in Q^h\}.
$$

We assume that the finite element pair (X^h, Q^h) satisfies the discrete inf-sup (or LBB) condition: There exists a constant $\beta > 0$, independent of h, such that

$$
\inf_{q^h\in Q^h} \sup_{v^h\in X^h} \frac{(q^h, \nabla \cdot v^h)}{\|\nabla v^h\|\|q^h\|} \geq \beta > 0,
$$

where β is a positive constant independent of the mesh size h. In addition, X^h and Q^h satisfy the approximation properties [5]:

$$
\begin{aligned}
&\inf_{v\in X^h} \|u - v\| \leq Ch^{k+1}\|u\|_{k+1}, \qquad v \in H^{k+1}(\Omega)^d, \\
&\inf_{v\in X^h} \|u - v\|_1 \leq Ch^k\|u\|_{k+1}, \qquad v \in H^{k+1}(\Omega)^d, \\
&\inf_{q\in Q^h} \|p - q\| \leq Ch^k\|p\|_k, \qquad p \in H^k(\Omega).
\end{aligned}
$$

The semidiscrete finite element approximation of (2.1) is: Find $u^h : [0, T] \to X^h$ and $p^h : [0, T] \to Q^h$ satisfy

$$
\begin{aligned}
&(u^h_t, v^h) + b(u^h, u^h, v^h) + \nu(\nabla u^h, \nabla v^h) - (p^h, \nabla \cdot v^h) = (f, v^h) \quad \forall v^h \in X^h, \\
&(\nabla \cdot u^h, q^h) = 0 \quad \forall q^h \in Q^h.
\end{aligned}
$$

The numerical discretization of the NS-α model requires an appropriate treatment of the differential filter. In the context of turbulence modeling, Germano [8] introduced the concept of a continuous differential filter.

Definition 2.1. Continuous differential filter: For $\phi \in L^2(\Omega)$ and $\alpha > 0$ is a fixed constant, denote the filter operation on ϕ by $\overline{\phi}$, where $\overline{\phi}$ is the unique solution of

$$
-\alpha^2\Delta\overline{\phi} + \overline{\phi} = \phi.
$$

Then, we define the discete differential filter from Kaya and Manica [13].

Definition 2.2. Discrete differential filter: For $w \in L^2(\Omega)$, for the filter radius $\alpha > 0, \overline{w}^h = (-\alpha^2\Delta + I)^{-1}w$ is the unique solution of

$$\alpha^2(\nabla\overline{w}^h, \nabla\psi) + (\overline{w}^h, \psi) = (w, \psi) \ \forall\psi \in X^h. \tag{2.2}$$

Now, we introduction some basic properties of discrete differential filters from [13].

Lemma 2.1. *For $w \in X$, we have the bound of the discretely filter and approximately w*

$$\|\overline{w}^h\| \leq \|w\|, \quad \|\nabla\overline{w}^h\| \leq \|\nabla w\|, \quad \|\nabla \times \overline{w}^h\| \leq \|\nabla w\|. \tag{2.3}$$

Proof. The proof of the first inequality in (2.3). Set $\psi = \overline{w}^h$ in (2.2), yielding

$$\alpha^2\|\nabla\overline{w}^h\|^2 + \|\overline{w}^h\|^2 = (w, \overline{w}^h) \leq \|w\|\|\overline{w}^h\|,$$

which directly implies $\|\overline{w}^h\| \leq \|w\|$.

For the second inequality in (2.3). Using the discrete Laplacian operator Δ^h defined by

$$-(\Delta^h\bar{w}^h, \psi) = (\nabla\bar{w}^h, \nabla\psi) \quad \forall\psi \in X^h,$$

we set $\psi = -\Delta^h\bar{w}^h$ in the rewritten filter equation to obtain

$$\alpha^2\|\Delta^h\bar{w}^h\|^2 + \|\nabla\bar{w}^h\|^2 = (\nabla w, \nabla\bar{w}^h) \leq \|\nabla w\|\|\nabla\bar{w}^h\|,$$

which yields $\|\nabla\bar{w}^h\| \leq \|\nabla w\|$.

For the third inequality in (2.3). By the vector identity for $v \in H^1(\Omega)^3$ with $v|_{\partial\Omega} = 0$,

$$\|\nabla \times v\|^2 + \|\nabla \cdot v\|^2 = \|\nabla v\|^2 + \text{boundary terms},$$

and since $\bar{w}^h$ satisfies homogeneous Dirichlet boundary conditions and is approximately divergence-free, we have $\|\nabla \times \bar{w}^h\| \leq \|\nabla\bar{w}^h\| \leq \|\nabla w\|$. □

The error analysis will use the discrete Gronwall's lemma:

Lemma 2.2. *Suppose that n and N are non-negative integers, $n \leq N$. The real numbers $a_n, b_n, c_n, \kappa_n, \Delta t, C$ are non-negative and satisfy that*

$$a_N + \Delta t\sum_{n=0}^{N} b_n \leq \Delta t\sum_{n=0}^{N-1}\kappa_n a_n + \Delta t\sum_{n=0}^{N} c_n + C.$$

Then,

$$a_N + \Delta t\sum_{n=0}^{N} b_n \leq \exp\left(\Delta t\sum_{n=0}^{N-1}\kappa_n\right)\left(\Delta t\sum_{n=0}^{N} c_n + C\right).$$

The proof of Lemma 2.2 can be found in [12].

Lemma 2.3. *If $u_t, u_{tt}, u_{ttt} \in L^2(0, T; H^k(\Omega))$, then we have the following inequalities*

$$\|u_{n+1} - 2u_n + u_{n-1}\|_k^2 \leq C(\Delta t)^3\int_{t_{n-1}}^{t_{n+1}}\|u_{tt}\|_k^2 dt,$$

$$\left\|\frac{3u_{n+1}-4u_n+u_{n-1}}{2\Delta t}\right\|_k^2 \le C\frac{1}{\Delta t}\int_{t_{n-1}}^{t_{n+1}}\|u_t\|_k^2 dt,$$
$$\left\|\frac{3u_{n+1}-4u_n+u_{n-1}}{2\Delta t}-u_t(t_{n+1})\right\|_k^2 \le C(\Delta t)^3\int_{t_{n-1}}^{t_{n+1}}\|u_{ttt}\|_k^2 dt.$$

We have used the following identity in the later proof

$$2(3a-4b+c,a)=|a|^2-|b|^2+|2a-b|^2-|2b-c|^2+|a-2b+c|^2. \tag{2.4}$$

3. Numerical scheme and its stability

In this section, we present the fully discrete BDF2 finite element scheme for the NS-α model and establish its unconditional stability. The scheme is derived as follows. Given $u_n^h, u_{n-1}^h \in V^h$, we extrapolate the convecting velocity to second-order accuracy as $2u_n^h - u_{n-1}^h \approx u(t_{n+1}) + O((\Delta t)^2)$. The BDF2 temporal discretization provides a second-order approximation of the time derivative. The resulting scheme reads: Find $(u_{n+1}^h, p_{n+1}^h) \in X^h \times Q^h$ such that for all $(v^h, q^h) \in X^h \times Q^h$,

$$\begin{aligned}&\frac{1}{2\Delta t}(3u_{n+1}^h-4u_n^h+u_{n-1}^h,v^h)+b_\alpha(2u_n^h-u_{n-1}^h,u_{n+1}^h,v^h)+\nu(\nabla u_{n+1}^h,\nabla v^h)\\&-(p_{n+1}^h,\nabla\cdot v^h)=(f_{n+1},v^h),\\&(\nabla\cdot u_{n+1}^h,q^h)=0.\end{aligned} \tag{3.1}$$

Here, the trilinear form $b_\alpha(2u_n^h-u_{n-1}^h,u_{n+1}^h,v^h)=((\nabla\times(2u_n^h-u_{n-1}^h))\times\overline{u_{n+1}^h}^h,v^h)$ corresponds to the rotational convective term in the continuous model (1.1).

Theorem 3.1. *Consider the NS-alpha model with the BDF2 scheme. A solution $u_n^l, l = 1,\cdots,M-1$, exists at each time-step. The scheme is unconditionally stable: The solution satisfy the following š¢ priori bound:*

$$\begin{aligned}&\|u_M^h\|^2+\|2u_M^h-u_{M-1}^h\|^2+2\nu\Delta t\sum_{n=1}^{M-1}\|\nabla u_{n+1}^h\|^2\\ \le&\frac{2\Delta t}{\nu}\sum_{n=1}^{M-1}\|f_{n+1}\|_*^2+\|u_1^h\|^2+\|2u_1^h-u_0^h\|^2.\end{aligned}$$

Proof. Set $v^h=\overline{u_{n+1}^h}^h$ in (3.1) and use the identity (2.4). The nonlinear term in the scheme vanishes. Thus, for every n we can obtain

$$\begin{aligned}&\frac{1}{4\Delta t}(\|u_{n+1}^h\|^2-\|u_n^h\|^2+\|2u_{n+1}^h-u_n^h\|^2-\|2u_n^h-u_{n-1}^h\|^2+\|u_{n+1}^h-2u_{n+1}^h+u_{n-1}^h\|^2)\\&+\nu\|\nabla u_{n+1}^h\|^2\leqslant\frac{1}{2\nu}\|f_{n+1}\|_*^2+\frac{\nu}{2}\|\nabla u_{n+1}^h\|^2,\end{aligned} \tag{3.2}$$

i.e.,

$$\frac{1}{2\Delta t}(\|u_{n+1}^h\|^2-\|u_n^h\|^2+\|2u_{n+1}^h-u_n^h\|^2-\|2u_n^h-u_{n-1}^h\|^2)+\nu\|\nabla u_{n+1}^h\|^2\leqslant\frac{1}{\nu}\|f_{n+1}\|_*^2. \tag{3.3}$$

Multiplying (3.3) by $2\Delta t$ and then summing it from $n = 1$ to $M - 1$, we have

$$\begin{aligned}&\|u_m^h\|^2 + \|2u_m^h - u_{m-1}^h\|^2 + 2\nu\Delta t \sum_{n=1}^{m-1} \|\nabla u_{n+1}^h\|^2 \\ \leq&\frac{2\Delta t}{\nu} \sum_{n=1}^{M-1} \|f_{n+1}\|_*^2 + \|u_1^h\|^2 + \|2u_1^h - u_0^h\|^2.\end{aligned}$$

□

Remark 3.1. Since the energy $E(u_n^h) := \frac{1}{2}\|u_n^h\|^2 + \frac{1}{2}\|2u_n^h - u_{n-1}^h\|^2$ and the energy dissipation $\varepsilon(u_n^h) := \nu\|\nabla u_n^h\|^2$ of NS-alpha model, we can get

$$E(u_M^h) + \nu\Delta \sum_{n=1}^{M-1} \varepsilon(u_{n+1}^h) = E(u_1^h) + \Delta t \sum_{n=1}^{M-1} (f_{n+1}, u_{n+1}^h). \tag{3.4}$$

Assume $\nu = 0$ and $f = 0$, we can get $E(u_M^h) = E(u_1^h)$. Hence, this scheme is energy conserving.

4. Error analysis

This section is devoted to a rigorous error analysis of the fully discrete scheme (3.1). We denote the error at time t_{n+1} by $e_{n+1} = u_{n+1} - u_{n+1}^h$. The main convergence result is stated in the following theorem.

Theorem 4.1. *Let (X^h, Q^h) be chosen as (P_2, P_1) TaylioršCHood elements, and further suppose that (u, p) is a solution of the NS-alpha model for $\alpha > 0, \nu > 0$, with given $f \in L^\infty(0, T; H^{-1}(\Omega))$, satisfies the following regularity*

$$u \in L^\infty(0, T; (H^{k+1}(\Omega)^d)), \quad u_t \in L^2(0, T; (H^{k+1}(\Omega)^d)), \tag{4.1}$$

$$u_{tt} \in L^2(0, T; (H^1(\Omega)^d)), \quad u_{ttt} \in L^2(0, T; (L^2(\Omega)^d)), \tag{4.2}$$

$$p \in L^2(0, T; H^{s+1}(\Omega)). \tag{4.3}$$

Then, (u_{n+1}^h, p_{n+1}^h) is given by method (3.1) with $n \in 1, 2, \cdots, m-1$, the error in the discrete solution satisfies

$$\frac{1}{2}\|e_m\|^2 + \nu\Delta t \sum_{n=1}^{m-1} \|\nabla e_{n+1}\|^2 \leq O(h^{2k} + \alpha^4 + (\Delta t)^4). \tag{4.4}$$

Proof. Note it for $u, v, w \in X$, we can define the filtering error accordingly:

$$FE = FE_\alpha(u, v, w) := ((\nabla \times u) \times (v - \bar{v}), w).$$

At time t_{n+1} the solution of the $NSE(u, p)$ satisfies,

$$\begin{aligned}&\frac{1}{2\Delta t}(3u_{n+1} - 4u_n + u_{n-1}, v^h) + b_\alpha(u_{n+1}, u_{n+1}, v^h) + \nu(\nabla u_{n+1}, \nabla v^h) \\ &- (p_{n+1}, \nabla \cdot v^h) \\ =&(f_{n+1}, v^h) + E_{n+1}^1(v^h) - FE(u_{n+1}, u_{n+1}, v^h),\end{aligned} \tag{4.5}$$

where $E^1_{n+1}(v^h)$ is denoted by

$$E^1_{n+1}(v^h) = (\frac{3u_{n+1} - 4u_n + u_{n-1}}{2\Delta t} - u_t(t_{n+1}), v^h).$$

We decompose the error as

$$e_{n+1} = \eta_{n+1} + \phi^h_{n+1}, \quad \eta_{n+1} = u_{n+1} - U_{n+1}, \quad \phi^h_{n+1} = U_{n+1} - u^h_{n+1}.$$

Here, U_{n+1} is the interpolation of u_{n+1} in V^h.

Subtracting (4.5) from (3.1), for all $(v^h, q^h) \in (X^h, Q^h)$, we have

$$\begin{aligned} &\frac{1}{2\Delta t}(3e_{n+1} - 4e_n + e_{n-1}, v^h) + \nu(\nabla e_{n+1}, \nabla v^h) - (p_{n+1} - p^h_{n+1}, \nabla \cdot v^h) \\ =& E^1_{n+1}(v^h) - E^2_{n+1}(v^h) - FE(u_{n+1}, u_{n+1}, v^h), \end{aligned} \tag{4.6}$$

where E^2_{n+1} is denoted by

$$E^2_{n+1} = b_\alpha(u_{n+1}, u_{n+1}, v^h) - b_\alpha(2u^h_n - u^h_{n-1}, u^h_{n+1}, v^h).$$

Setting $v^h = \phi^h_{n+1}$ in (4.6), we can get

$$\begin{aligned} &\frac{1}{2\Delta t}(3\phi^h_{n+1} - 4\phi^h_n + \phi^h_{n-1}, \phi^h_{n+1}) + \nu\|\nabla\phi^h_{n+1}\|^2 \\ =& -\frac{1}{2\Delta t}(3\eta_{n+1} - 4\eta_n + \eta_{n-1}, \phi^h_{n+1}) \\ &- \nu(\nabla\eta_{n+1}, \nabla\phi^h_{n+1}) + (p_{n+1} - \lambda^h_{n+1}, \nabla \cdot \phi^h_{n+1}) \\ &+ E^1_{n+1}(\phi^h_{n+1}) - E^2_{n+1}(\phi^h_{n+1}) - FE(u_{n+1}, u_{n+1}, \phi^h_{n+1}), \end{aligned} \tag{4.7}$$

for every $\lambda^h_{n+1} \in Q^h$, i.e.,

$$\begin{aligned} &\frac{1}{4\Delta t}(\|\phi^h_{n+1}\|^2 - \|\phi^h_n\|^2 + \|2\phi^h_{n+1} - \phi^h_n\|^2 - \|2\phi^h_n - \phi^h_{n-1}\|^2 + \|\phi^h_{n+1} - 2\phi^h_n + \phi^h_{n-1}\|^2) \\ &+ \nu\|\nabla\phi^h_{n+1}\|^2 \\ =& -\frac{1}{2\Delta t}(3\eta_{n+1} - 4\eta_n + \eta_{n-1}, \phi^h_{n+1}) - \nu(\nabla\eta_{n+1}, \nabla\phi^h_{n+1}) \\ &+ (p_{n+1} - \lambda^h_{n+1}, \nabla \cdot \phi^h_{n+1}) + E^1_{n+1}(\phi^h_{n+1}) - E^2_{n+1}(\phi^h_{n+1}) \\ &- FE(u_{n+1}, u_{n+1}, \phi^h_{n+1}), \end{aligned} \tag{4.8}$$

for every $\lambda^h_{n+1} \in Q^h$.

The terms on the right-hand side of (4.8) can be bounded as follows. $\forall \varepsilon_1 > 0$,

$$\begin{aligned} -\frac{1}{2\Delta t}(3\eta_{n+1} - 4\eta_n + \eta_{n-1}, \phi^h_{n+1}) &\le C\frac{1}{\Delta t}\|3\eta_{n+1} - 4\eta_n + \eta_{n-1}\|^2 + \epsilon_1\|\nabla\phi^h_{n+1}\|^2 \\ &\le C\frac{1}{\Delta t}\int_{t_{n-1}}^{t_{n+1}} \|\eta_t\|^2 dt + \varepsilon_1\|\nabla\phi^h_{n+1}\|^2, \end{aligned} \tag{4.9}$$

where we use the second inequality in lemma 2.3.

$$-\nu(\nabla\eta_{n+1}, \nabla\phi^h_{n+1}) \le \nu\|\nabla\eta_{n+1}\| \, \|\nabla\phi^h_{n+1}\|$$

$$\leq C\nu\|\nabla\eta_{n+1}\|^2 + \varepsilon_1\|\nabla\phi_{n+1}^h\|^2, \tag{4.10}$$

$$(p_{n+1} - \lambda_{n+1}^h, \nabla\cdot\phi_{n+1}^h) \leq C\|p_{n+1} - \lambda_{n+1}^h\|^2 + \varepsilon_1\|\nabla\phi_{n+1}^h\|^2. \tag{4.11}$$

For the term $E_{n+1}^1(\phi_{n+1}^h)$,

$$\begin{aligned} E_{n+1}^1(\phi_{n+1}^h) &= (\frac{3u_{n+1} - 4u_n + u_{n-1}}{2\Delta t} - u_t(t_{n+1}), \phi_{n+1}^h) \\ &\leq C\|\frac{3u_{n+1} - 4u_n + u_{n-1}}{2\Delta t} - u_t(t_{n+1})\|^2 + \|\phi_{n+1}^h\|^2 \\ &\leq C(\Delta t)^3\int_{t_{n-1}}^{t_{n+1}}\|u_{ttt}\|^2dt + \varepsilon_1\|\nabla\phi_{n+1}^h\|^2, \end{aligned} \tag{4.12}$$

where we use the third inequality in lemma 2.3.

Next, we bound the term $-E_{n+1}^2(\phi_{n+1}^h)$,

$$\begin{aligned} E_{n+1}^2(\phi_{n+1}^h) &= b_\alpha(u_{n+1}, u_{n+1}, \phi_{n+1}^h) - b_\alpha(2u_n^h - u_{n-1}^h, u_{n+1}^h, \phi_{n+1}^h) \\ &= b_\alpha(u_{n+1} - 2u_n + u_{n-1}, u_{n+1}, \phi_{n+1}^h) + b_\alpha(2e_n - e_{n-1}, u_{n+1}^h, \phi_{n+1}^h) \\ &\quad + b_\alpha(2u_n^h - u_{n-1}^h, \eta_{n+1}, \phi_{n+1}^h) \\ &= b_\alpha(u_{n+1} - 2u_n + u_{n-1}, u_{n+1}, \phi_{n+1}^h) + b_\alpha(2\eta_n - \eta_{n-1}, u_{n+1}^h, \phi_{n+1}^h) \\ &\quad + b_\alpha(2\phi_n^h - \phi_{n-1}^h, u_{n+1}^h, \phi_{n+1}^h) + b_\alpha(2u_n^h - u_{n-1}^h, \eta_{n+1}, \phi_{n+1}^h). \end{aligned} \tag{4.13}$$

$\forall\varepsilon_2, \varepsilon_3 > 0$, we have the following estimates.

$$\begin{aligned} b_\alpha(u_{n+1} - 2u_n + u_{n-1}, u_{n+1}, \phi_{n+1}^h) &\leq C\|\nabla(u_{n+1} - 2u_n + u_{n-1})\|\|\nabla\overline{u_{n+1}}^h\|\|\nabla\phi_{n+1}^h\| \\ &\leq C\|\nabla(u_{n+1} - 2u_n + u_{n-1})\|\|\nabla u_{n+1}\|\|\nabla\phi_{n+1}^h\| \\ &\leq C\|\nabla(u_{n+1} - 2u_n + u_{n-1})\|^2\|\nabla u_{n+1}\|^2 + \epsilon_1\|\nabla\phi_{n+1}^h\|^2 \\ &\leq C(\Delta t)^3\int_{t_{n-1}}^{t_{n+1}}\|\nabla u_{tt}\|^2dt\|u\|_{\infty,1}^2 + \varepsilon_1\|\nabla\phi_{n+1}^h\|^2, \end{aligned} \tag{4.14}$$

where we use the first inequality in lemma 2.3.

$$\begin{aligned} b_\alpha(2\eta_n - \eta_{n-1}, u_{n+1}^h, \phi_{n+1}^h) &\leq 2|b_\alpha(\eta_n, u_{n+1}^h, \phi_{n+1}^h)| + |b_\alpha(\eta_{n-1}, u_{n+1}^h, \phi_{n+1}^h)| \\ &\leq C\|\nabla\eta_n\|\|\nabla\overline{u_{n+1}^h}^h\|\|\nabla\phi_{n+1}^h\| + C\|\nabla\eta_{n-1}\|\|\nabla\overline{u_{n+1}^h}^h\|\|\nabla\phi_{n+1}^h\| \\ &\leq C\|\nabla\eta_n\|\|\nabla u_{n+1}^h\|\|\nabla\phi_{n+1}^h\| + C\|\nabla\eta_{n-1}\|\|\nabla u_{n+1}^h\|\|\nabla\phi_{n+1}^h\| \\ &\leq C(\|\nabla\eta_n\|^2 + \|\nabla\eta_{n-1}\|^2)\|\nabla u_{n+1}^h\|^2 + \varepsilon_1\|\nabla\phi_{n+1}^h\|^2, \end{aligned} \tag{4.15}$$

$$\begin{aligned} b_\alpha(2\phi_n^h - \phi_{n-1}^h, u_{n+1}^h, \phi_{n+1}^h) &\leq 2|b_\alpha(\phi_n^h, u_{n+1}^h, \phi_{n+1}^h)| + |b_\alpha(\phi_{n-1}^h, u_{n+1}^h, \phi_{n+1}^h)| \\ &\leq C\|\phi_n^h\|^{\frac{1}{2}}\|\nabla\phi_n^h\|^{\frac{1}{2}}\|\nabla\overline{u_{n+1}^h}^h\|\|\nabla\phi_{n+1}^h\| \\ &\quad + C\|\phi_{n-1}^h\|^{\frac{1}{2}}\|\nabla\phi_{n-1}^h\|^{\frac{1}{2}}\|\nabla\overline{u_{n+1}^h}^h\|\|\nabla\phi_{n+1}^h\| \\ &\leq C\|\phi_n^h\|^{\frac{1}{2}}\|\nabla\phi_n^h\|^{\frac{1}{2}}\|\nabla u_{n+1}^h\|\|\nabla\phi_{n+1}^h\| \\ &\quad + C\|\phi_{n-1}^h\|^{\frac{1}{2}}\|\nabla\phi_{n-1}^h\|^{\frac{1}{2}}\|\nabla u_{n+1}^h\|\|\nabla\phi_{n+1}^h\| \\ &\leq C\|\phi_n^h\|\|\nabla\phi_n^h\|\|\nabla u_{n+1}^h\|^2 \\ &\quad + C\|\phi_{n-1}^h\|\|\nabla\phi_{n-1}^h\|\|\nabla u_{n+1}^h\|^2 + \varepsilon_1\|\nabla\phi_{n+1}^h\|^2 \end{aligned}$$

$$
\begin{aligned}
&\le C\|\phi_n^h\|^2\|\nabla u_{n+1}^h\|^4 + C\|\phi_{n-1}^h\|^2\|\nabla u_{n+1}^h\|^4 \\
&\quad + \varepsilon_1\|\nabla\phi_{n+1}^h\|^2 + \varepsilon_2\|\nabla\phi_n^h\|^2 + \varepsilon_3\|\nabla\phi_{n-1}^h\|^2, \qquad (4.16)\\
b_\alpha(2u_n^h - u_{n-1}^h, \eta_{n+1}, \phi_{n+1}^h) &\le 2|b_\alpha(u_n^h, \eta_{n+1}, \phi_{n+1}^h)| + |b_\alpha(u_{n-1}^h, \eta_{n+1}, \phi_{n+1}^h)| \\
&\le C\|\nabla u_n^h\|\|\nabla\overline{\eta_{n+1}}^h\|\|\nabla\phi_{n+1}^h\| + C\|\nabla u_{n-1}^h\|\|\nabla\overline{\eta_{n+1}}^h\|\|\nabla\phi_{n+1}^h\| \\
&\le C(\|\nabla u_n^h\|^2 + \|\nabla u_{n-1}^h\|^2)\|\nabla\eta_{n+1}\|^2 + \varepsilon_1\|\nabla\phi_{n+1}^h\|^2. \qquad (4.17)
\end{aligned}
$$

Combining (4.14)-(4.17) with (4.13), we can get

$$
\begin{aligned}
-E_{n+1}^2(\phi_{n+1}^h) \le\, & C(\Delta t)^3\int_{t_{n-1}}^{t_{n+1}}\|\nabla u_{ttt}\|^2dt + C(\|\phi_n^h\|^2 + \|\phi_{n-1}^h\|^2) \\
& + C(\|\nabla\eta_n\|^2 + \|\nabla\eta_{n-1}\|^2) + C(\|\nabla u_n^h\|^2 + \|\nabla u_{n-1}^h\|^2)\|\nabla\eta_{n+1}\|^2 \\
& + 4\varepsilon_1\|\nabla\phi_{n+1}^h\|^2 + \varepsilon_2\|\nabla\phi_n^h\|^2 + \varepsilon_3\|\nabla\phi_{n-1}^h\|^2. \qquad (4.18)
\end{aligned}
$$

Next, we use the definition of the discrete filter to bound the filtering error

$$
\begin{aligned}
-FE &\le |((\nabla\times u_{n+1})\times(u_{n+1} - \overline{u_{n+1}}^h), \phi_{n+1}^h| \\
&\le C\|\nabla\times u_{n+1}\|\|\nabla(u_{n+1} - \overline{u_{n+1}}^h)\|\|\nabla\phi_{n+1}^h\| \\
&\le \varepsilon_1\|\nabla\phi_{n+1}^h\|^2 + C\alpha^4\|\nabla u_{n+1}\|^2\|\nabla\Delta^h\overline{u_{n+1}}^h\|^2 \\
&\le \varepsilon_1\|\nabla\phi_{n+1}^h\|^2 + C\alpha^4\|\nabla u_{n+1}\|^2\|u_{n+1}\|^2. \qquad (4.19)
\end{aligned}
$$

Set $\varepsilon_1 = \frac{1}{16}\nu, \varepsilon_2 = \frac{1}{8}\nu, \varepsilon_3 = \frac{1}{8}\nu$. From the mentioned above estimate (4.8)-(4.12), (4.18) and (4.19), we can get

$$
\begin{aligned}
&\frac{1}{4\Delta t}(\|\phi_{n+1}^h\|^2 - \|\phi_n^h\|^2 + \|2\phi_{n+1}^h - \phi_n^h\|^2 - \|2\phi_n^h - \phi_{n-1}^h\|^2 + \|\phi_{n+1}^h - 2\phi_n^h + \phi_{n-1}^h\|^2) \\
&\quad + \frac{1}{2}\nu\|\nabla\phi_{n+1}^h\|^2 - \frac{1}{8}\nu\|\nabla\phi_n^h\|^2 - \frac{1}{8}\nu\|\nabla\phi_{n-1}^h\|^2 \\
&\le C(\|\phi_n^h\|^2 + \|\phi_{n-1}^h\|^2) + C(\|\nabla\eta_{n+1}\|^2 + \|\nabla\eta_n\|^2 + \|\nabla\eta_{n-1}\|^2) \\
&\quad + C(\|\nabla u_n^h\|^2 + \|\nabla u_{n-1}^h\|^2)\|\nabla\eta_{n+1}\|^2 + \|p_{n+1} - \lambda_{n+1}^h\|^2 \\
&\quad + C\alpha^4\|\nabla u_{n+1}\|^2\|u_{n+1}\|^2 + C(\Delta t)^3\int_{t_{n-1}}^{t_{n+1}}\|u_{ttt}\|^2dt \\
&\quad + C\frac{1}{\Delta t}\int_{t_{n-1}}^{t_{n+1}}\|\eta_t\|^2dt + C(\Delta t)^3\int_{t_{n-1}}^{t_{n+1}}\|\nabla u_{tt}\|^2dt, \qquad (4.20)
\end{aligned}
$$

for every $\lambda_{n+1}^h \in Q^h$.

Multiplying (4.20) by $2\Delta t$ and summing it from $n = 1$ to $m - 1$, we have

$$
\begin{aligned}
&\frac{1}{2}\|\phi_m^h\|^2 + \frac{1}{2}\|2\phi_m^h - \phi_{m-1}^h\|^2 + \nu\Delta t\sum_{n=1}^{m-1}\|\nabla\phi_{n+1}^h\|^2 \\
&\le \frac{1}{2}\|\phi_1^h\|^2 + \frac{1}{2}\|2\phi_1^h - \phi_0^h\|^2 + C\Delta t\sum_{n=1}^{m-1}(\|\phi_n^h\|^2 + \|\phi_{n-1}^h\|^2) + \nu\frac{\Delta t}{4}\|\nabla\phi_1^h\|^2 \\
&\quad + \nu\frac{\Delta t}{4}\|\nabla\phi_0^h\|^2 + C\Delta t\sum_{n=1}^{m-1}(\|\nabla\eta_{n+1}\|^2 + \|\nabla\eta_n\|^2 + \|\nabla\eta_{n-1}\|^2)
\end{aligned}
$$

$$
\begin{aligned}
&+C\Delta t\sum_{n=1}^{m-1}(\|\nabla u_n^h\|^2+\|\nabla u_{n-1}^h\|^2)\|\nabla\eta_{n+1}\|^2+C\Delta t\sum_{n=1}^{m-1}\|p_{n+1}-\lambda_{n+1}^h\|^2\\
&+C\Delta t\sum_{n=1}^{m-1}\alpha^4\|\nabla u_{n+1}\|^2\|u_{n+1}\|^2+C\sum_{n=1}^{m-1}\int_{t_{n-1}}^{t_{n+1}}\|\eta_t\|^2dt\\
&+C(\Delta t)^4\sum_{n=1}^{m-1}\int_{t_{n-1}}^{t_{n+1}}\|u_{ttt}\|^2dt+C(\Delta t)^4\sum_{n=1}^{m-1}\int_{t_{n-1}}^{t_{n+1}}\|\nabla u_{tt}\|^2dt. \qquad (4.21)
\end{aligned}
$$

Applying lemma 2.2 to (4.21), we have

$$
\begin{aligned}
\frac{1}{2}\|\phi_m^h\|^2+\nu\Delta t\sum_{n=1}^{m-1}\|\nabla\phi_{n+1}^h\|^2 \le{}& C\|\phi_1^h\|^2+C\|2\phi_1^h-\phi_0^h\|^2\\
&+C\nu\Delta t\|\nabla\phi_1^h\|^2+C\nu\Delta t\|\nabla\phi_0^h\|^2\\
&+C\Delta t\sum_{n=1}^{m-1}(\|\nabla\eta_{n+1}\|^2+\|\nabla\eta_n\|^2+\|\nabla\eta_{n-1}\|^2)\\
&+C\Delta t\sum_{n=1}^{m-1}(\|\nabla u_n^h\|^2+\|\nabla u_{n-1}^h\|^2)\|\nabla\eta_{n+1}\|^2\\
&+C\Delta t\sum_{n=1}^{m-1}\|p_{n+1}-\lambda_{n+1}^h\|^2+C\Delta t\sum_{n=1}^{m-1}\alpha^4\|\nabla u_{n+1}\|^2\|u_{n+1}\|^2\\
&+C\sum_{n=1}^{m-1}\int_{t_{n-1}}^{t_{n+1}}\|\eta_t\|^2dt+C(\Delta t)^4\sum_{n=1}^{m-1}\int_{t_{n-1}}^{t_{n+1}}\|u_{ttt}\|^2dt\\
&+C(\Delta t)^4\sum_{n=1}^{m-1}\int_{t_{n-1}}^{t_{n+1}}\|\nabla u_{tt}\|^2dt. \qquad (4.22)
\end{aligned}
$$

Then, we bound the terms on the right-hand side of (4.22).

For the term $\sum_{n=1}^{m-1}\int_{t_{n-1}}^{t_{n+1}}\|\eta_t\|^2dt$, we have the following estimate

$$
\sum_{n=1}^{m-1}\int_{t_{n-1}}^{t_{n+1}}\|\eta_t\|^2dt\le Ch^{2k+2}\|u_t\|_{2,k+1}^2. \qquad (4.23)
$$

For the term $(\Delta t)^4\sum_{n=1}^{m-1}\int_{t_{n-1}}^{t_{n+1}}\|u_{ttt}\|^2dt$, we have the following estimate

$$
(\Delta t)^4\sum_{n=1}^{m-1}\int_{t_{n-1}}^{t_{n+1}}\|u_{ttt}\|^2dt\le C(\Delta t)^4\|u_{ttt}\|_{2,0}^2. \qquad (4.24)
$$

For the term $(\Delta t)^4\sum_{n=1}^{m-1}\int_{t_{n-1}}^{t_{n+1}}\|\nabla u_{tt}\|^2dt$, we have the following estimate

$$
(\Delta t)^4\sum_{n=1}^{m-1}\int_{t_{n-1}}^{t_{n+1}}\|\nabla u_{tt}\|^2dt\le C(\Delta t)^4\|u_{tt}\|_{2,1}^2. \qquad (4.25)
$$

For the term $\Delta t\sum_{n=1}^{m-1}(\|\nabla\eta_{n+1}\|^2+\|\nabla\eta_n\|^2+\|\nabla\eta_{n-1}\|^2)$, we have the following estimate

$$\begin{aligned}\Delta t\sum_{n=1}^{m-1}(\|\nabla\eta_{n+1}\|^2+\|\nabla\eta_n\|^2+\|\nabla\eta_{n-1}\|^2) &\le C\Delta t\sum_{n=0}^{m}\|\nabla\eta_n\|^2\\ &\le C\Delta t\sum_{n=0}^{m}h^{2k}\|u_n\|_{k+1}^2\\ &= Ch^{2k}|||u|||_{2,k+1}^2.\end{aligned}\tag{4.26}$$

For the term $\Delta t\sum_{n=1}^{m-1}(\|\nabla u_n^h\|^2+\|\nabla u_{n-1}^h\|^2)\|\nabla\eta_{n+1}\|^2$, we have the following estimate

$$\begin{aligned}\Delta t\sum_{n=1}^{m-1}(\|\nabla u_n^h\|^2+\|\nabla u_{n-1}^h\|^2)\|\nabla\eta_{n+1}\|^2 &\le Ch^{2k}\Delta t\sum_{n=1}^{m-1}(\|\nabla u_n^h\|^2+\|\nabla u_{n-1}^h\|^2)\|u_{n+1}\|_{k+1}^2\\ &\le Ch^{2k}|||u|||_{\infty,k+1}^2(\Delta t\sum_{n=0}^{m-1}\|\nabla u_n^h\|^2)\\ &\le Ch^{2k}|||u|||_{\infty,k+1}^2.\end{aligned}\tag{4.27}$$

For the term $\Delta t\sum_{n=1}^{m-1}\|p_{n+1}-\lambda_{n+1}^h\|^2$, λ_{n+1}^h is the interpolation of p_{n+1} in Q^h, we have the following estimate

$$\Delta t\sum_{n=1}^{m-1}\|p_{n+1}-\lambda_{n+1}^h\|^2\le Ch^{2s+2}|||p|||_{2,s+1}^2.\tag{4.28}$$

Combining (4.23)-(4.28) with (4.22)

$$\frac{1}{2}\|\phi_m^h\|^2+\nu\Delta t\sum_{n=1}^{m-1}\|\nabla\phi_{n+1}^h\|^2\le O(h^{2k}+\alpha^4+(\Delta t)^4).\tag{4.29}$$

Using the triangle inequality, we can get

$$\frac{1}{2}\|e_m\|^2+\nu\Delta t\sum_{n=1}^{m-1}\|\nabla e_{n+1}\|^2\le O(h^{2k}+\alpha^4+(\Delta t)^4).\tag{4.30}$$

We've done the proof. □

With the results, we can get that for the Taylor-Hood mixed finite element $k=2$, we can get the corollary.

Corollary 4.1. *Suppose that the finite element spaces X^h, Q^h are Taylor-Hood elements. Assume that the true solution (u,p) satisfies the regularity in Theorem (4.1) with $k=2$. Then, we can get the following estimate.*

$$|||e|||_{\infty,0}^2+|||\nabla e|||_{2,0}^2\le O(h^4+\alpha^4+(\Delta t)^4).\tag{4.31}$$

5. Numerical experiments

In this section, we present two numerical examples to validate the theoretical findings. The first example examines the convergence rates of the proposed scheme, while the second involves a benchmark problem of channel flow over a backward-facing step. In all experiments, we employ the Taylor–Hood finite element pair (P_2, P_1) for velocity and pressure. The computations are carried out using the finite element software FreeFEM++ [11].

5.1. Convergence rate verification

In order to verify the convergence rate of our scheme, we consider the NS-alpha model in unit square domain $\Omega = [0,1] \times [0,1]$ with the solution such that

$$\begin{aligned} u_1(x,y,t) &= (1+0.01t)\sin(2\pi y), \\ u_2(x,y,t) &= (1+0.01t)\cos(2\pi x), \\ p(x,y,t) &= x+y. \end{aligned}$$

In this test, we set $\nu = 1$, $T = 0.01$, and take the filtering radius α equal to the mesh size $h = 1/m$, where m denotes the number of uniform subdivisions in each spatial direction. Using (P_2, P_1) elements on uniformly refined meshes, we compute the numerical errors and the corresponding convergence rates. The results for the NS-α model are listed in Table 1. The observed rates agree well with the theoretical predictions.

Table 1. Error and convergence rates for NS-alpha.

m	Δt	$\|\|\|u-u^h\|\|\|_{\infty,0}$	Rate	$\|\|\|\nabla u - \nabla u^h\|\|\|_{2,0}$	Rate	$\|\|\|p-p^h\|\|\|_{2,0}$	Rate
8	T/2	3.3981e-2		1.0822e-2		5.5981e-2	
16	T/4	1.0762e-2	1.658	2.7421e-3	1.980	1.4082e-2	1.990
32	T/8	3.1901e-3	1.754	6.8903e-4	1.992	3.5321e-3	1.995
64	T/16	8.9633e-4	1.831	1.7266e-4	1.997	8.8453e-4	1.995

5.2. Variable-step BDF2 test

To demonstrate the robustness of the scheme with non-uniform time steps, we conduct a numerical experiment with variable Δt. The time step is adaptively chosen based on the local truncation error estimate, with $\Delta t_{\min} = T/16$ and $\Delta t_{\max} = T/4$. The results confirm that the second-order convergence rate is preserved under mild variations in the time step size, with the error remaining comparable to the uniform step case. This validates the potential for adaptive time-stepping strategies, whose rigorous analysis will be pursued in future work.

5.3. Channel flow over a step

In the second experiment, we simulate the two-dimensional channel flow over a backward-facing step using the BDF2 scheme for the NS-α model. The computational domain Ω is a $[0,40]\times[0,10]$ rectangle with a 1×1 step located on the bottom wall for $x \in [5,6]$. No-slip boundary conditions are imposed on the top and bottom walls as well as on the step surface. At the inlet (left boundary) and outlet (right boundary), we prescribe the following parabolic velocity profile

$$\begin{aligned} u_1(0,y) &= u_1(40,y) = \frac{y(10-y)}{25}, \\ u_2(0,y) &= u_2(40,y) = 0. \end{aligned}$$

The flow is driven by a kinematic viscosity of $\nu = 1/600$ from left to right, with no external force ($f = 0$). The time step is set to $\Delta t = 0.01$, and the simulation runs until $T = 40$. Two meshes are employed: A coarse mesh and a fine mesh, illustrated in Figures 1 and 2, respectively. The coarse mesh contains 24,544 degrees of freedom, while the fine mesh has 41,322. Under these conditions, we expect the formation and subsequent detachment of vortices downstream of the step.

First, we compute the flow by directly solving the Navier–Stokes equations using the same (P_2, P_1) Taylor–Hood elements and the BDF2 time-stepping scheme. The velocity field at $T = 40$ is shown in Figure 3. While the solution remains smooth, it fails to capture the vortex shedding and reattachment phenomena accurately.

A central objective of turbulence modeling is to achieve physically faithful predictions on coarser grids than those required for direct numerical simulation (DNS). To this end, we apply the NS-α model on the coarse mesh, keeping all other parameters identical to the NSE simulation. The NS-α model not only yields a smooth velocity field but also correctly reproduces the vortex dynamics behind the step.

Figure 4 displays the velocity magnitude obtained with the NS-α model on the coarse mesh at $T = 40$, with filtering radius $\alpha = 0.125$. The results confirm that the NS-α model successfully captures both the formation and detachment of eddies downstream of the step, maintaining physical realism while using a significantly coarser discretization compared to DNS of the NSE.

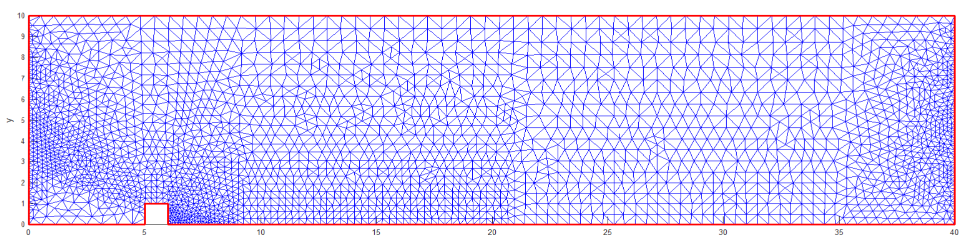

Figure 1. Two-dimensional channel flow over a step, coarse mesh.

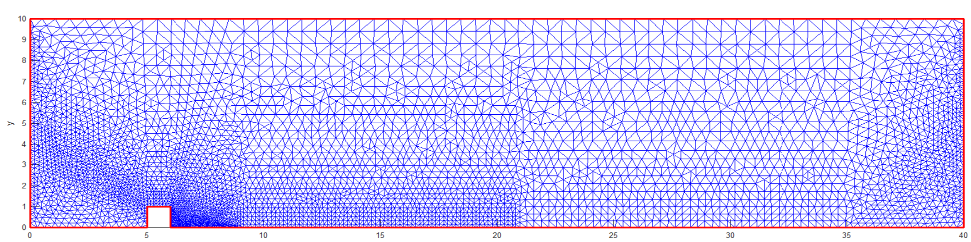

Figure 2. Two-dimensional channel flow over a step, fine mesh.

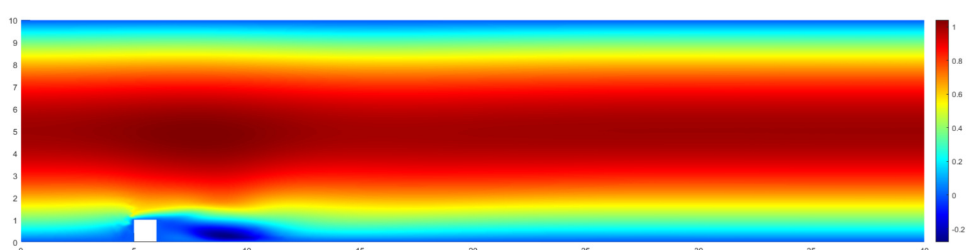

Figure 3. Navier-Stokes equations on the fine mesh, T=40, $\nu = 1/600$.

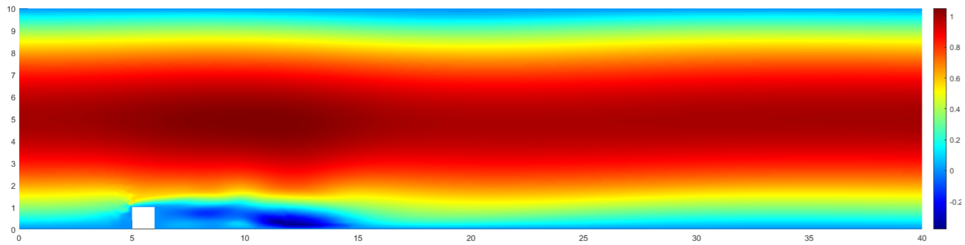

Figure 4. NS-alpha model on the coarse mesh, T=40, $\nu = 1/600$, $\alpha = 0.125$.

6. Conclusion

In this paper, we have developed and analyzed a fully discrete numerical scheme for the NS-α model in $\mathbb{R}^d$ $(d = 2, 3)$ with no-slip boundary conditions, combining the second-order backward differentiation formula (BDF2) for time discretization with finite elements in space. A complete numerical analysis has been presented, establishing the unconditional stability of the scheme and deriving optimal-order error estimates. Theoretical results confirm that the discrete solutions converge to the true solution of the Navier–Stokes equations under appropriate regularity assumptions. The validity of the analysis is supported by several numerical experiments.

Future work will focus on extending the proposed framework to a broader range of applications and enhancing its computational efficiency. For instance, incorporating projection or pressure-correction techniques, as well as employing the generalized scalar auxiliary variable (GSAV) approach, could further improve stability and facilitate the simulation of more complex flows. The analysis of variable-step BDF2 methods, which offer greater flexibility in adaptive time-stepping strategies, will be pursued in subsequent studies. Recent developments [4, 22] have established stability and error estimates for variable-step BDF2 schemes applied to diffusion and Navier-Stokes equations. The extension of these techniques to the NS-α model, which involves additional complexity due to the filtering operation and the rotational nonlinear term, represents an important direction for future research.

Declarations

Conflict of interest. The authors declare that they have no conflict of interest.

Data availability. No data was used or generated in the paper.

Acknowledgment. The authors would like to thank the referees for valuable comments and suggestions in improving this article.

Funding. Not applicable.

References

[1] R. A. Adams and J. J. F. Fournier, *Sobolev Spaces*, Elsevier, Amsterdam, 2003.

[2] M. Akbas, S. Kaya and L. G. Rebholz, *On the stability at all times of linearly extrapolated BDF2 timestepping for multiphysics incompressible flow problems*, Numer. Meth. Part. D. E., 2017, 33(4), 999–1017.

[3] G. Akrivis and B. Y. Li, *Error estimates for fully discrete BDF finite element approximations of the Allen–Cahn equation*, IMA J. Numer. Anal., 2021, 42(1), 363–391.

[4] B. García-Archilla and J. Novo, *Robust error bounds for the Navier–Stokes equations using implicit-explicit second-order BDF method with variable steps*, IMA J. Numer. Anal., 2023, 43(5), 2892–2933.

[5] S. C. Brenner and L. R. Scott, *The Mathematical Theory of Finite Element Methods*, Springer, New York, 2008.

[6] J. S. Dokken, A. Johansson, A. Massing and S. W. Funke, *A multimesh finite element method for the Navier–Stokes equations based on projection methods*, Comput. Methods Appl. Mech. Engrg., 2020, 368, 113129.

[7] E. Fried and M. E. Gurtin, *Turbulent kinetic energy and a possible hierarchy of length scales in a generalization of the Navier-Stokes α theory*, Phys. Rev. E, 2007, 75(5), 056306.

[8] M. Germano, *Differential filters for the large eddy numerical simulation of turbulent flows*, Phys. Fluids, 1986, 29(6), 1755–1757.

[9] V. Girault and P. A. Raviart, *Finite Element Methods for Navier-Stokes Equations: Theory and Algorithms*, Springer-Verlag, New York, 1986.

[10] J. L. Guermond, J. T. Oden and S. Prudhomme, *An interpretation of the Navier–Stokes-alpha model as a frame-indifferent Leray regularization*, Physica D, 2003, 177(1–4), 23–30.

[11] F. Hecht, *New development in FreeFem++*, J. Numer. Math., 2012, 20(3–4), 1–14.

[12] J. G. Heywood and R. Rannacher, *Finite-element approximation of the nonstationary Navier–Stokes problem. Part IV: Error analysis for second-order time discretization*, SIAM J. Numer. Anal., 1990, 27(2), 353–384.

[13] S. Kaya and C. C. Manica, *Convergence analysis of the finite element method for a fundamental model in turbulence*, Math. Models Methods Appl. Sci., 2012, 22(11), 1250033.

[14] A. N. Kolmogorov, *The local structure of turbulence in incompressible viscous fluid for very large Reynolds numbers*, Proc. R. Soc. Lond. A: Math. Phy., 1991, 434(1890), 9–13.

[15] W. Layton, C. C. Manica, M. Neda and L. G. Rebholz, *Numerical analysis and computational comparisons of the NS-alpha and NS-omega regularizations*, Comput. Methods Appl. Mech. Engrg., 2010, 199(13–16), 916–931.

[16] W. Layton, L. Rebholz and M. Sussman, *Energy and helicity dissipation rates of the NS-alpha and NS-alpha-deconvolution models*, IMA J. Appl. Math., 2010, 75(1), 56–74.

[17] W. Layton, I. Stanculescu and C. Trenchea, *Theory of the NS-ω model: A complement to the NS-α model*, Commun. Pur. Appl. Anal., 2011, 10(6), 1763–1777.

[18] M. Lesieur, O. Métais and P. Comte, *Large-Eddy Simulations of Turbulence*, Cambridge university press, Cambridge, 2005.

[19] Y. Li and R. An, *Error analysis of an unconditionally stable BDF2 finite element scheme for the incompressible flows with variable density*, J. Sci. Comput., 2023, 95(3), 73.

[20] Y. Li, J. Li, L. Q. Mei and Y. P. Li, *Mixed stabilized finite element methods based on backward difference/Adams–Bashforth scheme for the time-dependent variable density incompressible flows*, Comput. Math. Appl., 2015, 70(10), 2575–2588.

[21] X. Li, J. Shen and Z. Liu, *New SAV-pressure correction methods for the Navier-Stokes equations: Stability and error analysis*, Math. Comp., 2022, 91(333), 141–167.

[22] H. L. Liao and Z. M. Zhang, *Analysis of adaptive BDF2 scheme for diffusion equations*, Math. Comp., 2021, 90(329), 1207–1226.

[23] E. Lunasin, S. Kurien, M. A. Taylor and E. S. Titi, *A study of the Navier–Stokes-α model for two-dimensional turbulence*, J. Turbul., 2007, 8, N30.

[24] W. W. Miles and L. G. Rebholz, *An enhanced-physics-based scheme for the NS-α turbulence model*, Numer. Meth. Part. D. E., 2010, 26(6), 1530–1555.

[25] S. S. Ravindran, *A second-order backward difference time-stepping scheme for penalized Navier–Stokes equations modeling filtration through porous media*, Numer. Meth. Part. D. E., 2016, 32(2), 681–705.

[26] L. Rebholz and F. Tone, *Long-time H^1-stability of BDF2 time stepping for 2D Navier–Stokes equations*, Appl. Math. Lett., 2023, 141, 108624.

[27] Y. Rong and J. A. Fiordilino, *Numerical analysis of a BDF2 modular grad–div stabilization method for the Navier–Stokes equations*, J. Sci. Comput., 2020, 82(3), 66.

[28] J. Wang, M. Li and Y. Zhang, *Superconvergence analysis of BDF-Galerkin FEM for nonlinear Schrödinger equation*, Numer. Algorithms, 2022, 89(1), 195–222.

Received December 2025; Accepted March 2026; Available online July 2026.